buildings

MDPI

Article

Effectiveness of Selected Strain and Displacement Measurement Techniques in Civil Engineering

Piotr Szewczyk [1,*] and Piotr Kudyba [2]

[1] Faculty of Civil and Environmental Engineering, West Pomeranian University of Technology Szczecin, al. Piastów 17, 70-310 Szczecin, Poland
[2] FRONESIS Marek M. Kudyba, al. Wyzwolenia 57/11, 71-400 Szczecin, Poland; kudybapiotr@gmail.com
* Correspondence: szewczyk@zut.edu.pl

Abstract: The aim of this study was to assess how useful certain selected measurement techniques are in civil engineering. In this work, the focus was placed on the measurement of displacement and strain. Classical methods with an established position in the industry, such as electrical resistance strain gauge measurements and linear variable differential transducers (LVDT), were compared with modern techniques that do not require direct contact with the measured object, such as laser scanning and digital image correlation. A simply supported beam was bent in two types of tests. In the first test, a small load was applied on the beam, causing a slight deflection of the structure of approximately 0.5 mm. This enabled us to assess how effective the tested methods were, given the very precise measurement of the structure. In the second test, a much higher load was introduced, which caused displacement that can realistically be found in actual civil engineering structures. Ultimately, the model went through the plastic phase and was damaged. This enabled the measurement of displacement and strain that were much higher than those of the safe operating range of the structure. Based on conducted examinations, practical conclusions were drawn relative to the analyzed measurement methods.

Keywords: digital image correlation; 3D laser scanner; LVDT transducers; strain gauges

check for updates

Citation: Szewczyk, P.; Kudyba, P. Effectiveness of Selected Strain and Displacement Measurement Techniques in Civil Engineering. *Buildings* **2022**, *12*, 172. https://doi.org/10.3390/buildings12020172

Received: 28 December 2021
Accepted: 1 February 2022
Published: 3 February 2022

Publisher's Note: MDPI stays neutral with regard to jurisdictional claims in published maps and institutional affiliations.

Copyright: © 2022 by the authors. Licensee MDPI, Basel, Switzerland. This article is an open access article distributed under the terms and conditions of the Creative Commons Attribution (CC BY) license (https://creativecommons.org/licenses/by/4.0/).

1. Introduction

Measurement is an inherent element of a civil engineer's work. Measurement is made in construction commissioning, load tests of, e.g., bridges, as well as in expert evaluation of a construction, property survey or structural failure. Linear, horizontal and vertical displacements are usually measured. However, one can also analyze angular displacement, displacement velocity and acceleration. In recent years, diagnostics of building structures based on modal analysis has also been developing [1,2]. Strain measurement is an interesting problem. Owing to the character and stiffness of civil engineering structures, strain is usually small and does not exceed 1–2 per mills. Therefore, precise measurement instruments need to be used. Strain measurement allows one more possibility. Given that the examined structure operates in the elastic regime and if the Young's modulus of the material is known, it is possible to determine stress resulting from the applied load. If the geometric characteristics of the cross-section are known, the bending moment or axial force can also be determined.

Structure measurement can be conducted using many tools. Some of them have been successfully used in the industry for years, e.g., linear variable differential transducers (LVDTs). They are used in many types of industry. They can function as separate sensors or as components of other devices. They can be elements of production control or device diagnostics. They come in a very wide range of measuring lengths. In civil engineering, they perform excellently in model tests, expert opinions and test loads. Simple mechanical displacement sensors can also be applied successfully in many situations. For example,

when a measurement is made out in the open, providing power can be a problem. Another classical solution for strain measurement is to use electrical resistance strain gauges, although optical strain gauges (also known as fiber optic strain sensors) and vibrating-wire jointmeters are becoming increasingly popular. Strain gauges, thanks to the connection with the tested object, enable the implementation of extremely precise measurements in industry. It can be used even on small or curved surfaces or in dynamic tests. Using strain gauges, transducers are also built, e.g., for force or torque.

Modern measurement techniques that do not require direct contact with the measured object provide an alternative to traditional methods. No contact gives some advantage, but it also poses some limitations. Laser scanning is a technique that is getting to be more popular. It can very well be applied for structural engineering surveying and for the measurement of objects with either complicated geometry or where access is limited [3,4]. This technique is also used in architecture and monument conservation. In combination with photogrammetry, it enables precise reproduction of even very complex geometry. The laser beam must bounce back from the examined object and return to the scanner. However, some methods do not require any contact with the measured object, e.g., digital image correlation (DIC). The method relies on analyzing a series of pictures taken of the measured object. The object is photographed by two cameras placed at a certain angle to each other. This type of image acquisition, just like in the case of human vision, enables spatial analysis of the structure. This method is gaining more and more applications in many industries. An interesting application is production control, where quality can be assessed by comparing the measurement with the reference model. These measurements are carried out both on production lines and measurements of individual products, e.g., in shipyards when verifying the geometry of the ship sections. Thanks to the use of high-speed cameras, it is possible to measure dynamic processes, e.g., car crash tests or crack propagation in the tested material.

There are many works comparing different measurement methods in the literature [5–14]. The aim of the work was to compare the usefulness of the above methods for measurement operations in civil engineering. Given the example of a simple beam structure, analysis was performed to determine which method can be applied for the precise measurement of displacement and strain and which method failed to meet expectations.

2. Models and Methods

2.1. Experimental Model

As the main aim of the study was to assess the effectiveness of a measurement carried out with different methods, a decision was made to make the research model simple, to make the interpretation of results easier.

A steel beam, presented in Figure 1, was used for the study. It was a simply supported beam with the distance between supports of 3200 mm (full length was 3400 mm). The cross-section consisted of two C260 profiles welded so that they made a closed section. As the cross-section is characterized with high torsional stiffness, it eliminated the risk of buckling when bending. Load was placed in the middle of the beam using a Zwick/Roell hydraulic actuator with a range of 600 kN, controlled by ControlCube servo controller and Cubus software. The HBM MGCplus data system and Catman/Easy software were used for data acquisition. Moreover, thanks to the use of an analog output in the MGCplus measurement cards, the signal of force and displacement transducers and strain gauges was connected to the measurement system using the digital image correlation method.

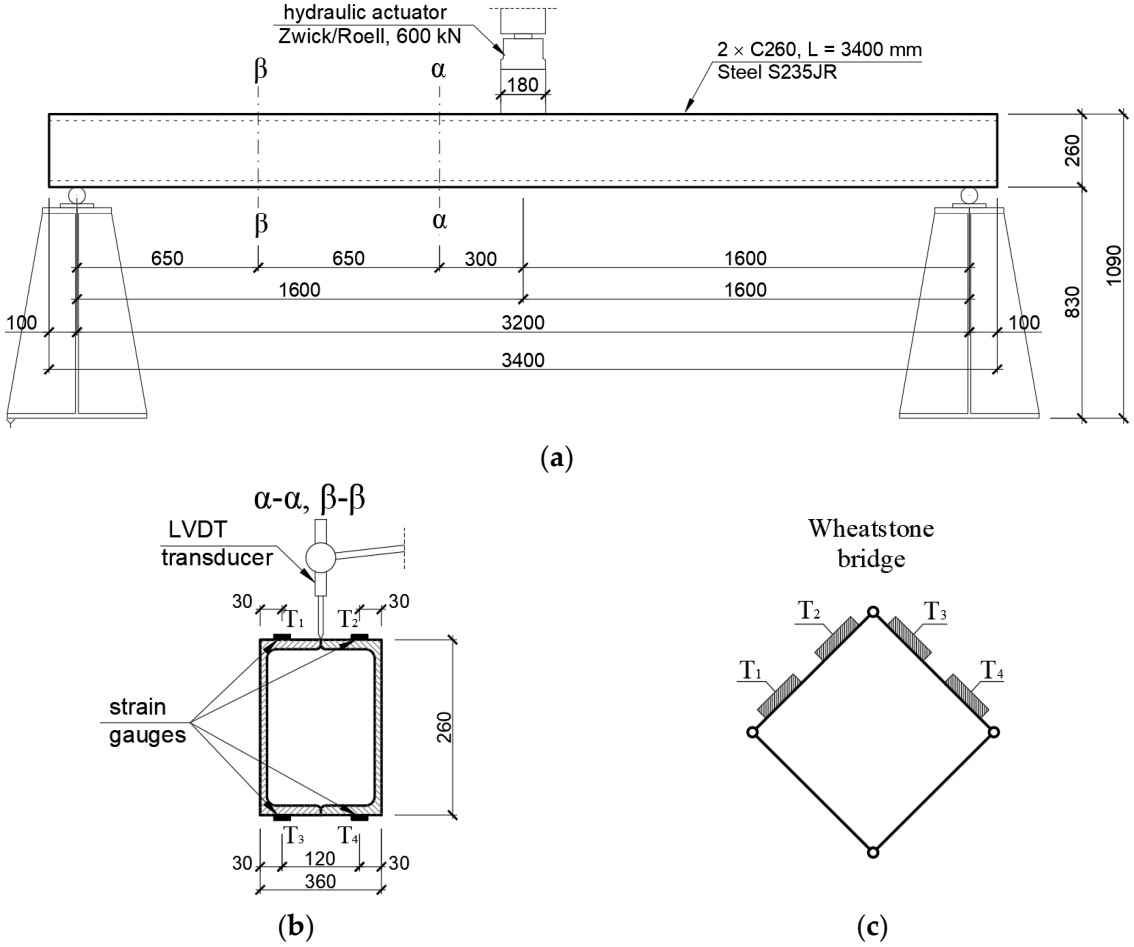
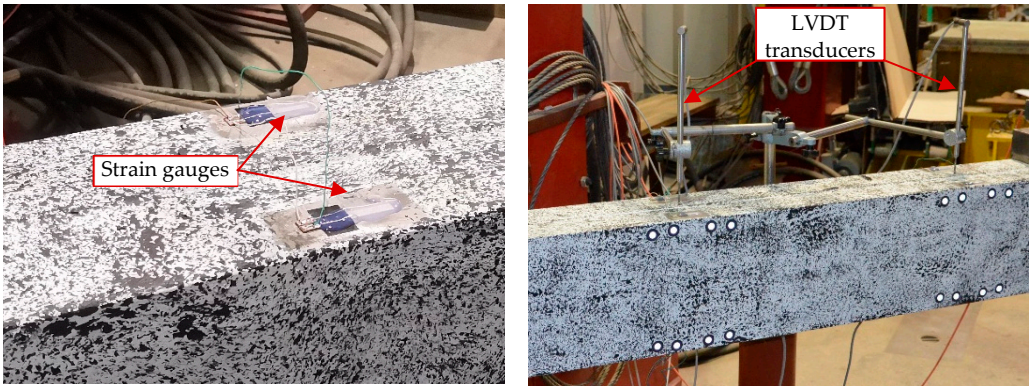


Figure 1. Scheme of the test stand: (**a**) view of the tested beam; (**b**) location of measurement sensors in the cross-section; (**c**) location of strain gauges in the Wheatstone bridge.

Two measurement cross-sections, α-α and β-β, were determined on the beam. Their precise location is shown in Figure 1. Displacement and strain were measured in each cross-section with different instruments. The below sections present their short characteristics. As the available body of literature on the applied measurement methods is very extensive, focus was placed on obtained results, rather than on detailed description.

2.2. Electrical Resistance Strain Gauges (SGs)

An electrical resistance strain gauge is a classic device used to precisely measure strain. It will take advantage of resistance change resulting from the gauge changing its length while it is attached to the structure. Electrically, the gauge measures the potential difference in an electrical circuit known as a Wheatstone bridge [15]. Figure 1b shows the cross-section of the beam together with the location of four strain gauges, and Figure 2a shows the gauges glued to the upper flange. Gauges with a measurement base of 15 mm and a resistance of 120 Ω were used. Figure 1c shows the Wheatstone bridge scheme. As half bridge configurations were used, the signal from all four gauges summed up into one measurement point.



(**a**) (**b**)

Figure 2. Measuring sensors: (**a**) electrical resistance strain gauges; (**b**) LVDT transducers.

2.3. Linear Variable Differential Transformer (LVDT Transducers)

A classic device used for displacement measurement is the linear variable differential transformer (LVDT), as shown in Figure 2b. Two sensors were used: one for measuring vertical displacement in α-α cross-section and the other in β-β cross-section. The location of the sensor in the transverse section is presented in Figure 1b. The device has a core that slides inside a coil causing a voltage change proportional to the core's displacement. HBM WA/200 mm-L transducers with a measurement range of 200 mm were used in the study. A displacement of 200 mm is equivalent to a voltage change of 80 mV/V.

2.4. Digital Image Correlation (DIC-3D)

While taking a measurement with an LVDT requires contact with the examined object, a non-contact alternative does exist, namely, ARAMIS SRX 3D camera system manufactured by GOM that uses digital image correlation method. The device instantaneously takes a sequence of pictures of the investigated object with two cameras that are arranged to each other at a preset angle.

Two cameras with 4K resolution were placed on the measuring beam at 1600 mm distance. The angle of value 20 was included between the axes of these two cameras. As a result, a measuring volume with a range of 3890 × 3100 × 3100 mm was created. The tripod with cameras was about 4000 mm in front of the tested object. Aramis Professional 2020 software was used for the measurement, and the GOM Correlate 2020 software was used to analyze the data.

The human brain creates a 3D image based on analysis of images provided by a pair of eyes. DIC system works in a similar way. To make a measurement, it is required to locate the same fragment of a structure with two cameras. For this purpose, a special pattern is applied to the tested object [16,17]. This pattern is created by black spots on a matte white paint covering the entire test object. The size of the spots depends on the measuring volume used. The proportion between the surface covered with black spots and the white undercoat is also important, it should be even. The algorithms contained in the measurement software are able to locate the same range of the complicated pattern on two cameras. Consequently, it enables 3D analysis of linear and angular displacement in all six degrees of freedom.

Figure 3 shows the examined beam covered in the pattern. It is also possible to track the displacement of selected points—stickers are used as measurement markers to this end (Figure 2b, Figure 3 and Figure 21a). These markers were applied to the strain measurements. On this basis, extensometers were created. This has been described in more detail in Section 3.4.

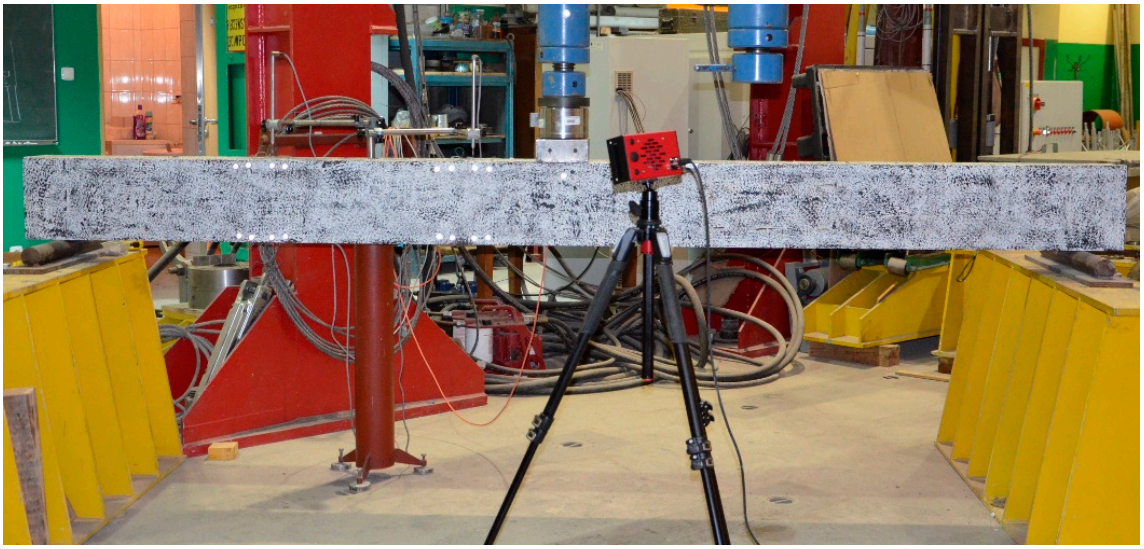


Figure 3. View of the tested beam covered with a black and white pattern.

In the case of testing steel structures, the possibility of taking measurements during welding is also important [18–22]. It is required to use appropriate filters, but due to the lack of contact with the tested object, there is no risk of damaging the measuring sensor.

2.5. 3D Laser Scanner

Laser scanning is another non-contact method used for measuring structures [23–25]. The laser generates a beam of light that bounces back from the object and returns to the device. The phase shift of light that returns to the scanner compared to the phase of light that leaves it is measured. The difference is proportional to the distance between the object and the scanner. When the shift is known, this distance can be calculated. A FARO Focus S70 (Figure 4) scanner was used in the experiments.



Figure 4. View of the FARO Focus S70 scanner.

When a scanner is used, measurement time is of importance. Time depends on scan resolution, i.e., density of data points. The more measurements are made, the more accurate

the final effect. Of course, this approach means longer measurement time and more data collected. The FARO Focus S70 scanner has 9 resolution settings, as presented in Table 1.

Table 1. Examples of FARO Focus S70 scanner operation modes.

Distance: 10 m		Distance: 5 m	
Scan Resolution	**Dot Grid Density [mm]**	**Scan Resolution**	**Dot Grid Density [mm]**
1/1	1.5	1/1	0.8
1/2	3.1	1/2	1.6
1/4	6.1	1/4	3.1
1/5	7.7	1/5	3.8
1/8	12.3	1/8	6.2
1/10	15.3	1/10	7.6
1/16	24.5	1/16	12.3
1/20	30.7	1/20	15.4
1/32	49.1	1/32	24.6

For example, if the scanner is placed 10 m away from the examined object, the highest and the lowest resolution will produce a mesh size of 1.5 mm and almost 50 mm, respectively. If the scanner is 5 m away from the object, the respective figures are 0.75 and 24.5 mm. The second factor that affects measurement time is the angle at which the scan is made. Measurement is possible within the whole 360 degrees. However, if you limit the angle, the measuring time will be significantly reduced. On the other hand, restricting the measurement range will also reduce the number of measurements. All of these factors were taken into account while taking measurements in the study.

3. Results

3.1. Research Scope

Research was divided into two main parts. In part one, the usefulness of measurement equipment for relatively small displacement values typical in civil engineering was measured. In part two, the load was gradually increased and ultimately the models entered plastic range and were damaged. That allowed us to analyze the behavior of sensors given the large displacement. Displacement and strain were measured in α-α and β-β cross-sections using all available methods.

3.2. Displacement Measurement

In the first test, load was gradually increased so that vertical displacement in the α-α cross-section increased by 0.5 mm. After each load change, constant force was maintained for some time. Three steps were complete, which was equivalent to a displacement of 1.5 mm. Displacement in the whole experiment was measured with an LVDT and DIC system. The latter is able to measure all analyzed data points at the same time. A graphic interpretation of results is also possible by creating displacement mapping. An example of such a map is shown in Figure 5. Results for the α-α cross-section are presented in Figure 6. Disturbance that is visible at each displacement increase is linked to PID control hydraulic actuators.

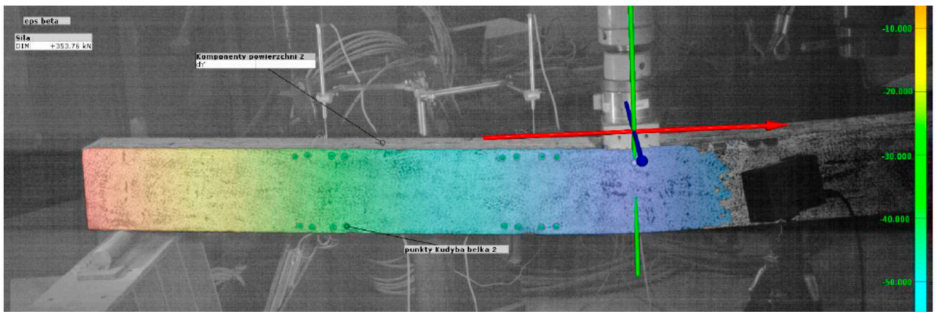


Figure 5. An exemplary map of vertical displacements of the analyzed beam.

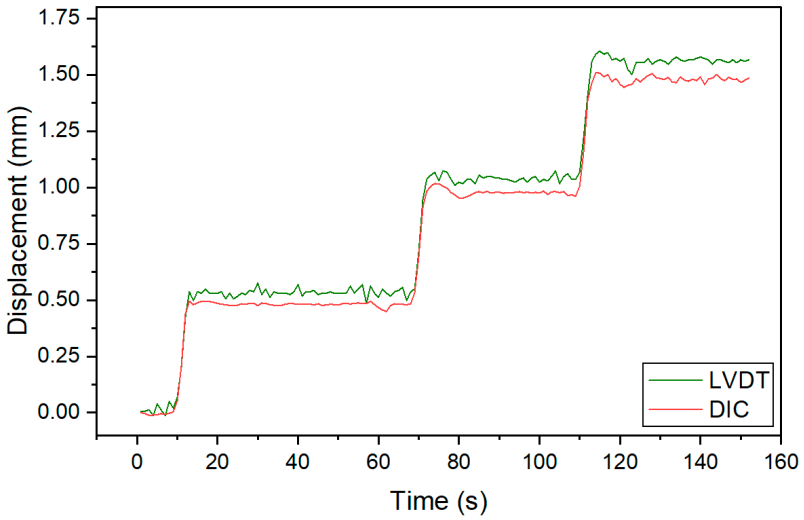


Figure 6. Comparison of the results of vertical displacements in the α-α section.

After each load change, there was a stability period during which measurement was taken with laser scanner. Tables 2 and 3 show a range of data obtained for different distances between the scanner and the object, the applied angle and resolution. No clear effect of the scanning settings on the obtained results was observed. The main factor that generated a measurement error was noise detected in data point clouds. Although the noise can be eliminated by manual analysis of the scan, it is time consuming.

Table 2. Displacements from a distance of 5 m measured with the laser scanner.

	Scan Angle: 10°			Scan Angle: 5°			Command
Scan Resolution	**1/4**	**1/2**	**1/1**	**1/4**	**1/2**	**1/1**	
displacement [mm]	0.00	0.00	0.00	0.00	0.00	0.00	0.0
	−0.48	−0.33	−0.41	−0.62	−0.45	−0.46	0.5
	−0.97	−0.95	−1.07	−1.22	−1.01	−1.03	1.0
	−1.47	−1.31	−1.47	−1.66	−1.51	−1.48	1.5

Table 3. Displacements from a distance of 10 m measured with the laser scanner.

	Scan Angle: 10°		Scan Angle: 5°		Command
Scan Resolution	**1/2**	**1/1**	**1/2**	**1/1**	
displacement [mm]	0.00	0.00	0.00	0.00	0.0
	−0.49	−0.56	−0.40	−0.46	0.5
	−0.92	−1.14	−0.90	−0.95	1.0
	−1.49	−1.64	−1.48	−1.50	1.5

Figure 7 shows a comparison of all three methods. The results are presented as the beam's static equilibrium path. It is the effect of load acting on the beam on displacement in the α-α cross-section. The results recorded in a continuous manner are shown as solid lines. The results of the scanner measurement from Tables 2 and 3 are given as points.

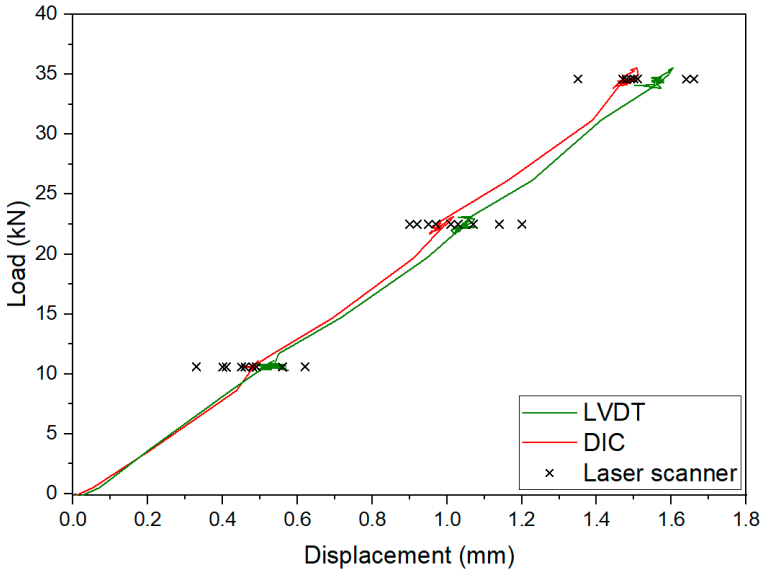


Figure 7. Static equilibrium path of the tested beam in the elastic range of displacements.

The analysis of results showed that all applied methods of displacement measurement brought positive effects. In most cases, the difference in measurement was less than 0.1 mm, which in the context of construction is good enough.

The next step was to test the performance of sensors in a broader range of displacement. To this end, load was placed on the beam so that displacement in the α-α cross-section increased incrementally by approximately 2 mm. When the beam in its middle cross-section started to enter plastic range, increase increment went up to 4 mm. When plastic deformation was visible, the increment increased to 16 mm. The results are presented in Figure 8. The LVDT and DIC system took measurements continuously (the solid line). Measurements with the laser scanner, just like before, were taken when a constant load was applied. The results are given as points in a graph.

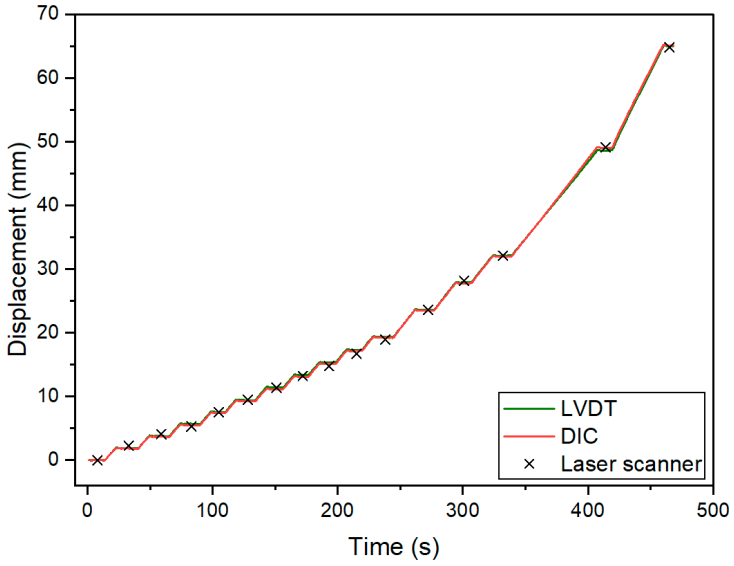


Figure 8. Comparison of the results of vertical displacements in the α-α section.

Results are also presented as the beam's static equilibrium path (Figure 9). It is the effect of load acting on the beam on displacement in the α-α cross-section. The results discussed in Section 3.2 demonstrate that the accuracy of all measurement techniques was good enough and that they can be used to measure displacement in construction work [26–30].

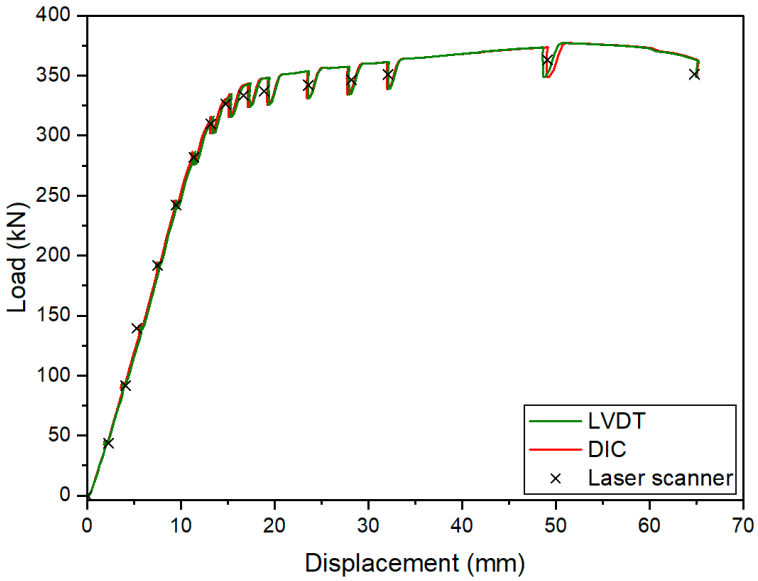


Figure 9. Static equilibrium path of the tested beam in the plastic range of displacements.

3.3. Determination of Beam Deflection Line

The laser scanner and DIC system, respectively, scan and photograph the examined object. It allows one to analyze data of any part of the object. At this point, an attempt was made to determine the beam deflection line based on measurements taken before.

DIC systems can be used to draw any line and generate a graph relative to it. A horizontal line in Figure 10 was generated. A curve of vertical displacement (Figure 11) was generated relative to the line. Although the generated curve has some slight disturbance, its shape is in line with expectations.

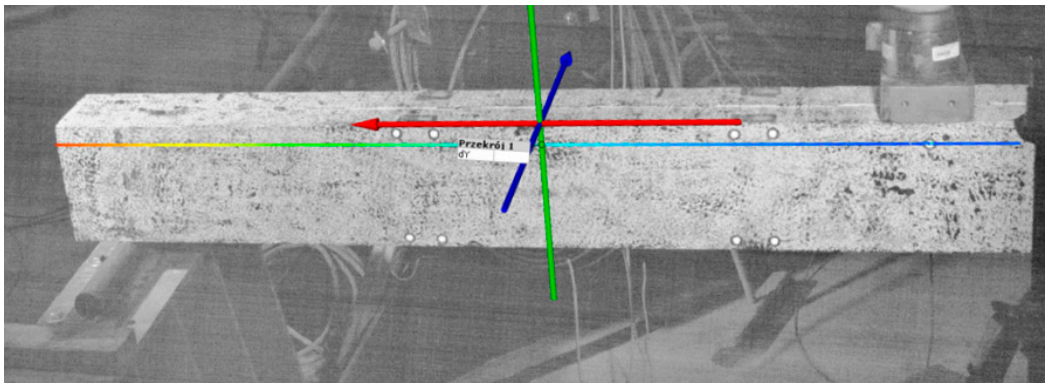


Figure 10. The line along which the deflection line plot was created.

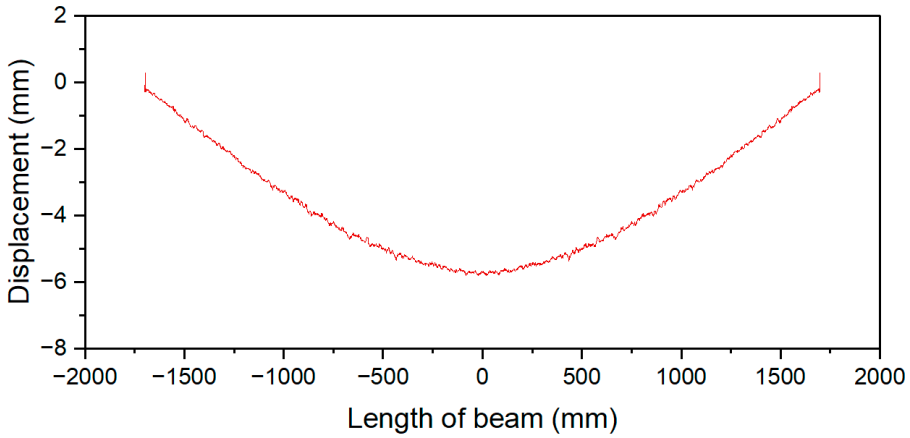


Figure 11. Deflection line created in the DIC system.

Next, the performance of the laser scanner was tested in its ability to generate the deflection line of the scanned object. Figure 12 shows the side plane of the beam after scanning.

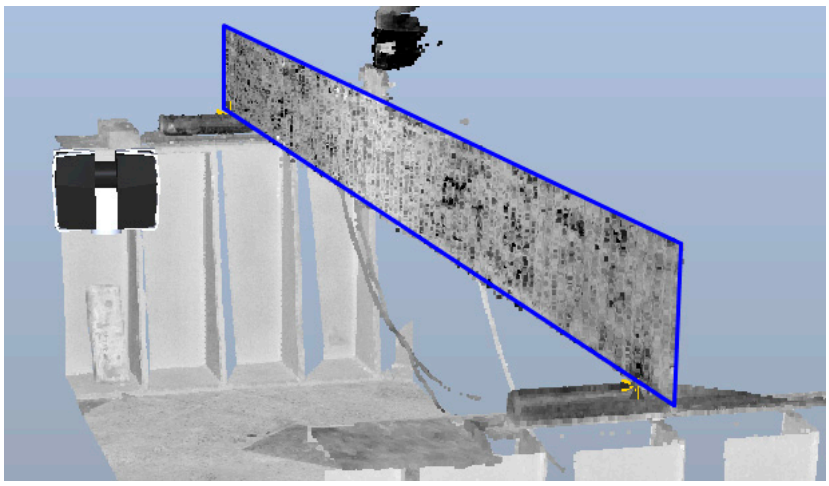


Figure 12. Side plane of the beam after scanning.

First, software provided by the scanner's manufacturer was used. Some 35 × 45 mm areas separated by 320 mm were determined on the scanned beam (Figure 13). Vertical displacement was determined for each area and then the data were used to generate the deflection line in Figure 14.

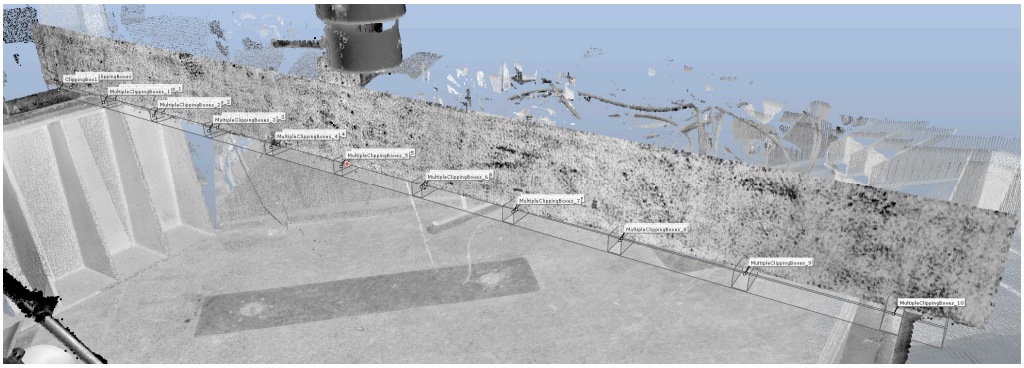


Figure 13. Arrangement of displacement measurement areas.

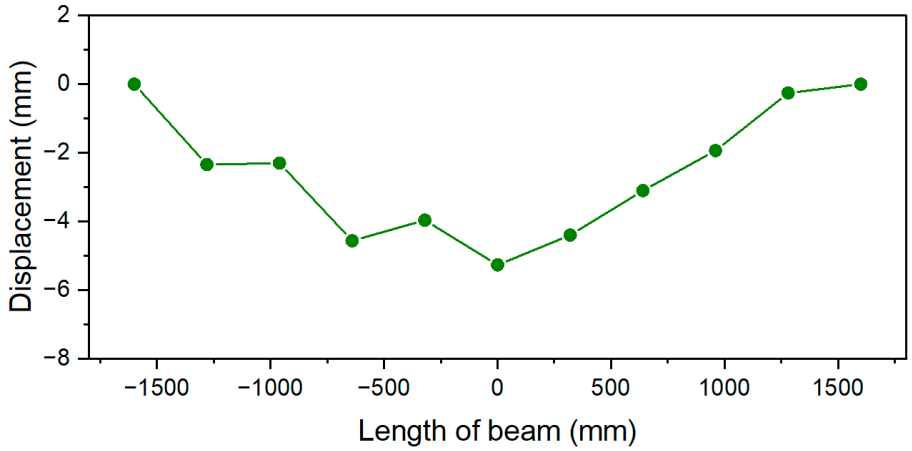


Figure 14. Deflection line created by scanning.

Maximum displacement is consistent with measurement taken with the other methods. Unfortunately, the generated shape of the deflection line is unsatisfactory. It can be due to the instability of measurement made at the edge of the element. The beam of light that hits the edge would often bounce in an uncontrolled way. This results in blank spaces and noise. This effect is presented in Figure 15, which shows a point cloud generated using measurement data. The red line represents the edge of the element.

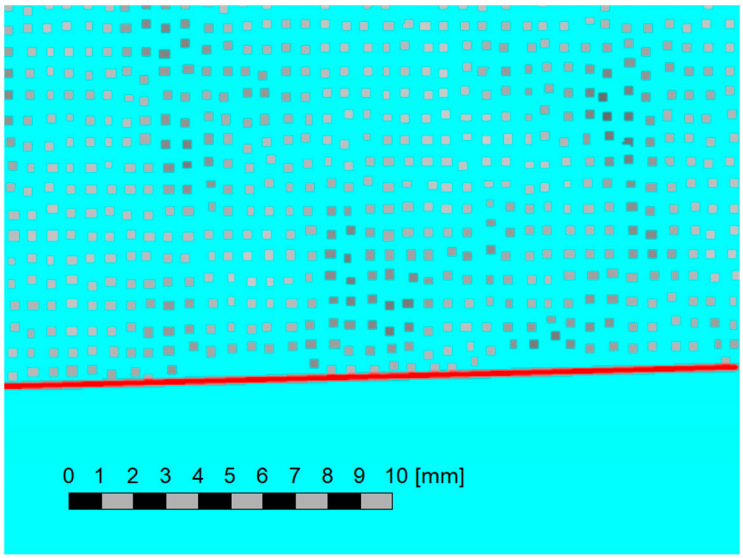


Figure 15. Cloud of points on the edge of the element.

Next, an algorithm was developed that would divide the beam into elementary units of the same length. The algorithm sought the smallest vertical coordinates in each part and placed it in a graph. Figure 16 shows examples of automatically generated curves. All curves describe the same deflection of the beam. The length of elementary unit was different for each curve in the range of 1–320 mm.

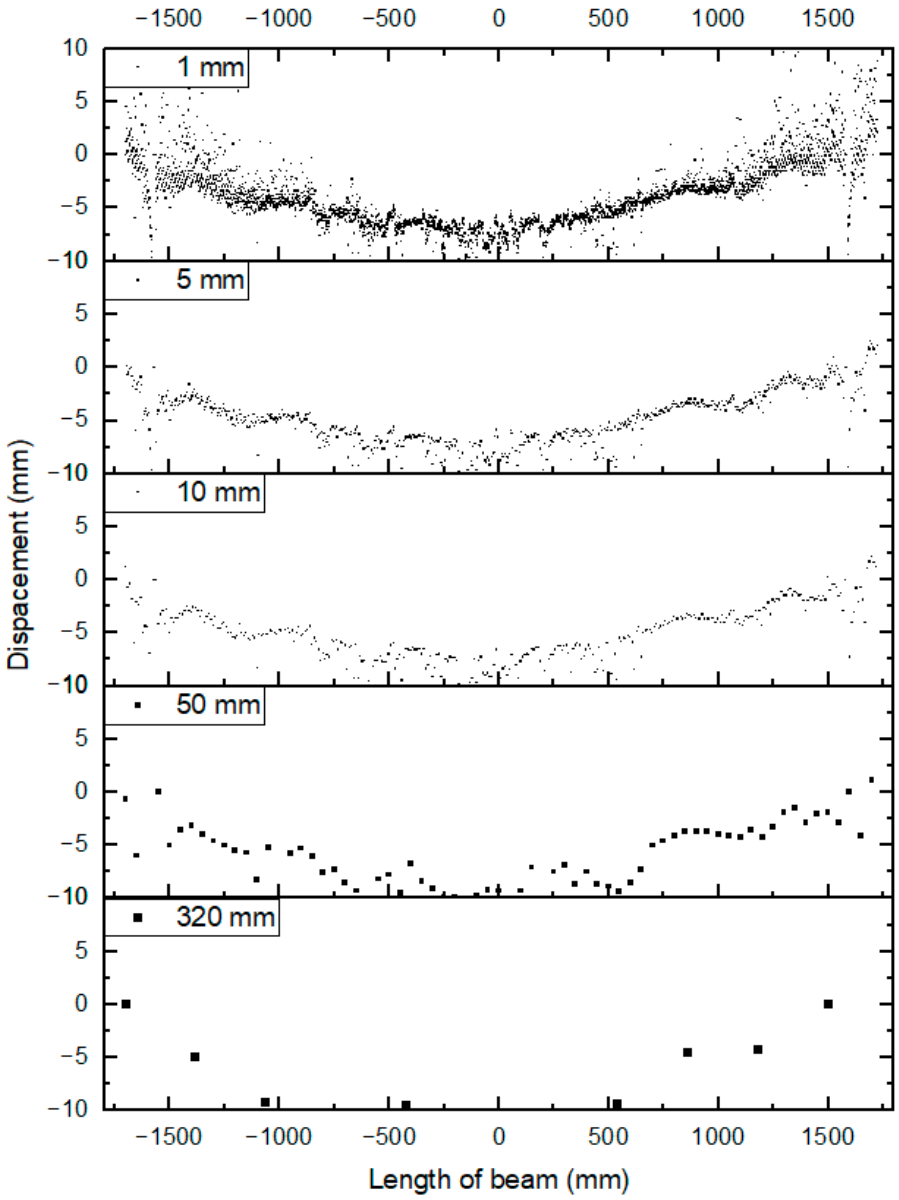


Figure 16. Deflection lines created by scanning at different measuring section lengths (1–320 mm).

One problem one faces in the automatic generation of a deflection line is that it is impossible to remove noise in the scan in a simple way. The verification of whether any given data point was measured correctly or was just a result of the laser beam bouncing in an uncontrollable way definitely complicates automatic curve generation. Consequently, the obtained results are strongly correlated to the length of the measured part.

Figure 17 shows a comparison of obtained data. DIC-generated deflection lines are compared with those determined in the manual processing of data points and a selected automatically generated line. The DIC system performed better than other systems. Because of noise, measurement with laser scanning is less accurate.

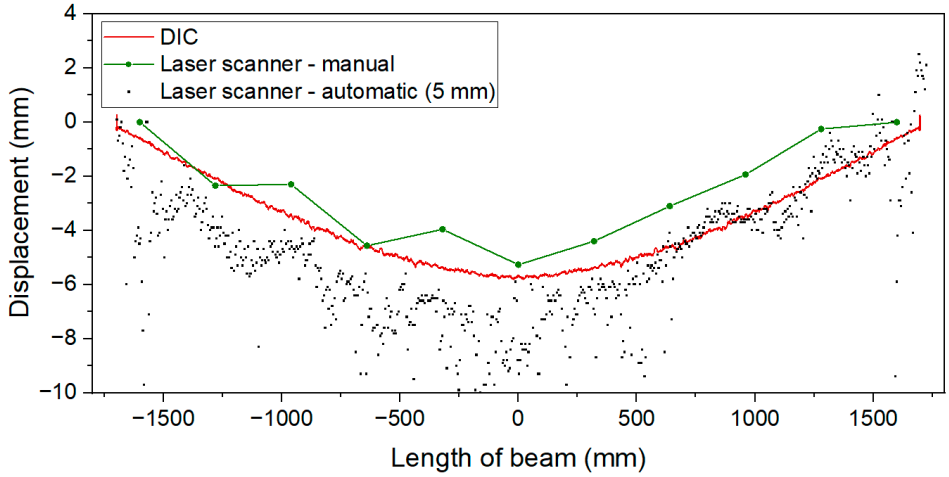


Figure 17. Comparison of deflection lines obtained with different methods.

The location of the scanner relative to the examined object is of great importance for the quality of displacement measurement. In the analyzed case, the beam deflection line was generated in the plane parallel to beam deflection direction (the side of the beam), as shown in Figure 12. The quality of data can be improved by positioning the scanner so that displacement measurement would happen in the plane perpendicular to beam deflection direction (bottom or top of the beam). In our case, it would require placing the scanner distinctly below or above the beam. Unfortunately, it was not possible in the conducted experiment.

3.4. Strain Measurement

Because civil engineering structures are very stiff, strain measurement requires more precision than the measurement of displacement. The strain gauge is a classic device used for strain measurement. Electrical resistance strain gauges were used in the research. Their positioning in measured cross-sections is presented in Figures 1 and 2.

An attempt was also made to measure strain with the other two, non-contact methods. The laser scanner does not have a dedicated tool for measuring strain. It was assumed that strain measurement will be conducted by measuring distance change between points superimposed on the examined object. A punch was used to make four points with a diameter of 2 mm in the α-α cross-section. The assumed point distribution allowed us to create extensometers with a measurement base of 100 and 200 mm (Figure 18).

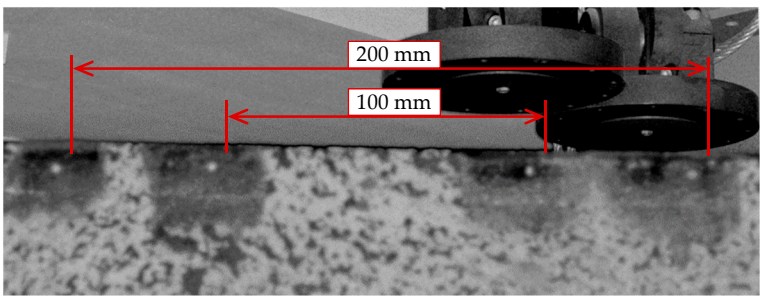
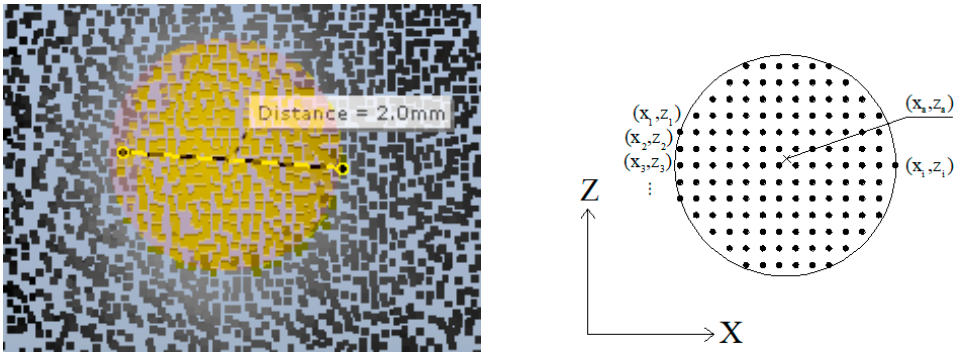


Figure 18. Distribution of points to create an extensometer.

To achieve better accuracy, the points were scanned only at the distance of 300 mm, with the highest resolution. As a result, point mesh with a size of approximately 0.05 mm was obtained. The first step was to determine the coordinates in the middle of the measurement point by selecting points within the 2 mm diameter mark (Figure 19a). The scanner's software supplied by the manufacturer enables one to export the coordinates of each point to a text file. Then, MS Excel was used to determine the average coordinate in

the X (along the beam's axis) and Z directions (beam's vertical displacement), as shown in Figure 19b.



(**a**) (**b**)

Figure 19. Point cloud within the measuring point: (**a**) selection of points; (**b**) determining the center of the circle as the measuring point.

Having determined the precise position of points, the distances between them were measured and thus a measurement base with a length of approximately 100 and 200 mm was created. Then, load was introduced and the changes of distances between the points were measured. Unfortunately, despite many attempts, measurement taken with this method produced variable results and was finally thought not to be reliable.

The DIC system allows one to analyze strain with two methods. First, the whole area covered with a pattern is analyzed. Strain can be displayed in two perpendicular directions. Figure 20 shows examples of strain maps in the direction parallel to the beam's axis. The first figure shows strain before load introduction. The successive two figures present strain maps in the beam's elastic regime. Figure 20b,c show the moment when a load of 105 and 245 kN is applied to the beam, causing strain in the α-α cross-section of 0.45‰ and 1.06‰, respectively. Figure 20d demonstrates the moment the beam enters its nonlinear operation at the load of 285 kN and strain of 1.26‰. Figure 20e shows the state at maximum load-bearing capacity at 365 kN, with strain in the α-α cross-section of 2.0‰. For a better interpretation of the presented strain maps, they should be analyzed in combination with Figure 9 that shows the beam's static equilibrium path.

The method of load introduction very clearly divides the beam into the compressed zone above its neutral axis and the tensile zone below it. Unfortunately, the division cannot be seen in the obtained strain maps. It is only when plastic deformation occurs, caused by load introduction, that a clear division between the two zones can be seen. The division is visible at a large increase in strain that definitely exceeds strain typical for civil engineering members.

The second method of measuring strain in a DIC system is to create virtual extensometers between the predefined points. To this end, special measurement markers were glued and thus four extensometers were created (Figure 20a); two with a measurement base of 100 mm and two with a base of 200 mm. The extensometers were prepared to take measurements both at the top (Figure 20b) and bottom (Figure 20c) parts of the cross-section. Extensometers with a measurement base of 100 and 200 mm were created at slightly different levels in the cross-section, as shown in Figure 21. This is due to the limitations of the DIC system, which will not perform the correct measurement with three points on one line. These differences in measurements were corrected with the results presented in the following figures.

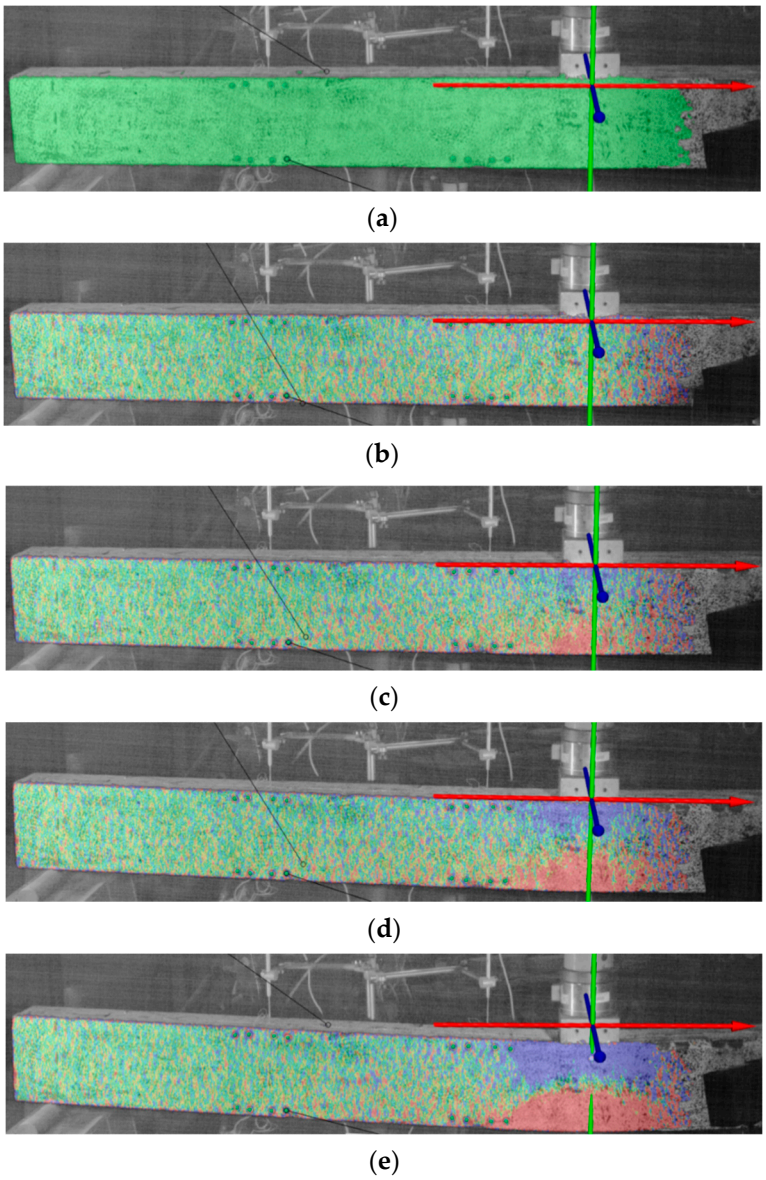
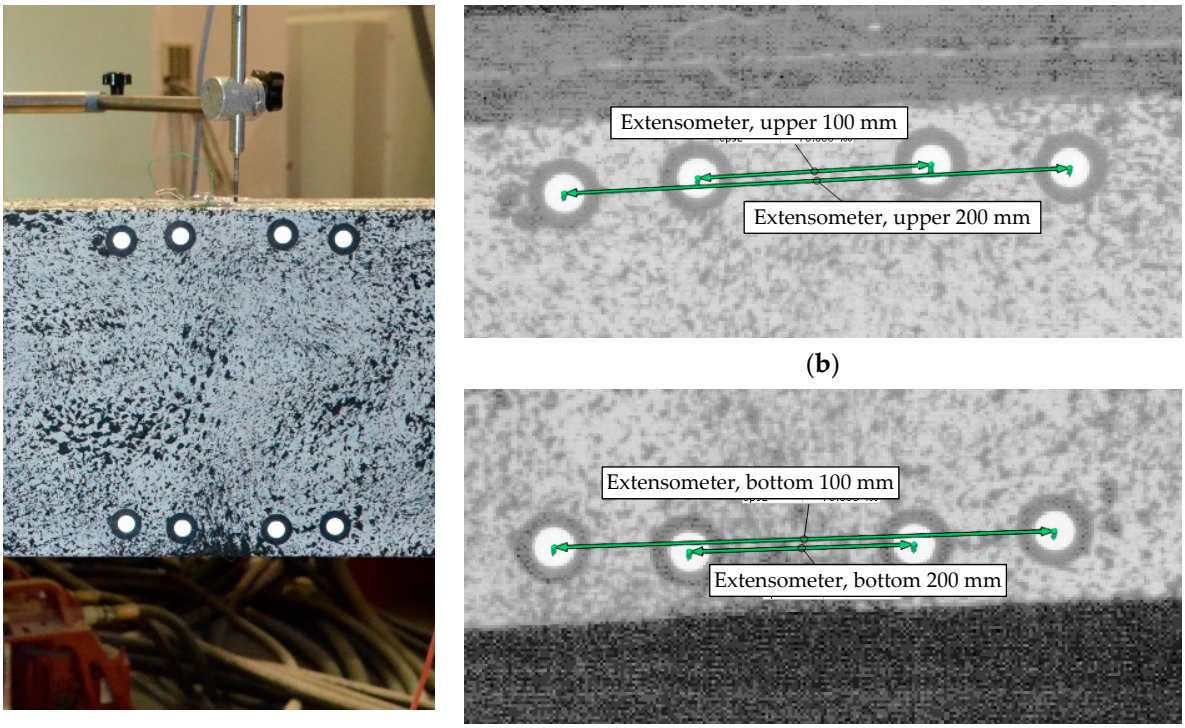


Figure 20. Strain maps in the direction parallel to the beam's axis: (**a**) no load; (**b**) load: 105 kN; (**c**) load: 245 kN; (**d**) load: 285 kN; (**e**) load: 365 kN.



(**a**) (**b**) (**c**)

Figure 21. Extensometers created in the DIC system: (**a**) view of measurement markers; (**b**) extensometers at the top of the section; (**c**) extensometers at the bottom of the section.

First, measurements in the elastic range were made, with vertical displacement in the α-α cross-section increasing by 0.5 mm increments (displacement curve in Figure 6). Figure 22 compares strain in the α-α cross-section measured with the strain gauge and with DIC-generated extensometers. Unfortunately, measurements made with a DIC system are characterized by a significant scatter. The scatter is many orders of magnitude greater than the measured values. Strain measurement with digital image correlation did not prove to be reliable.

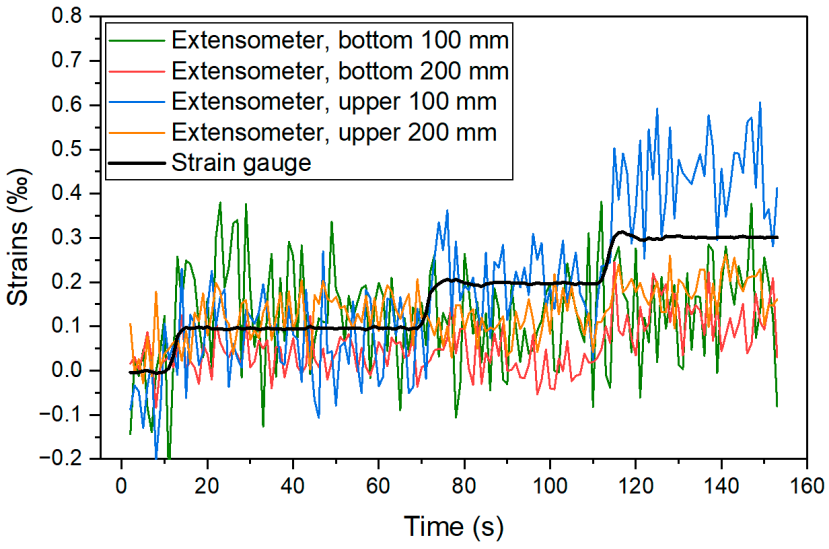


Figure 22. Comparison of the strain measurements in the elastic range in the α-α section.

Then, the results obtained in the test when the beam was damaged were compared. Relevant displacement results are presented in Figures 8 and 9. Figure 23 shows a com-

parison of strain measured in the α-α cross-section close to plastic deformation. Figure 24 presents results for the β-β cross-section where strain stabilizes despite an increasing load acting on the beam. The effect is due to the formation of plastic deformation in the middle of the beam's span. At higher strain, measurement results obtained with the two compared methods converge. Nevertheless, measurement taken with the DIC system is characterized with a large dispersion of measured values. The scatter shown in Figures 23 and 24 reaches 0.5‰. Bearing in mind that for a steel beam a strain change of 0.5‰ corresponds to a stress change of over 100 MPa, obtained measurements cannot be recommended for analysis of civil engineering structures.

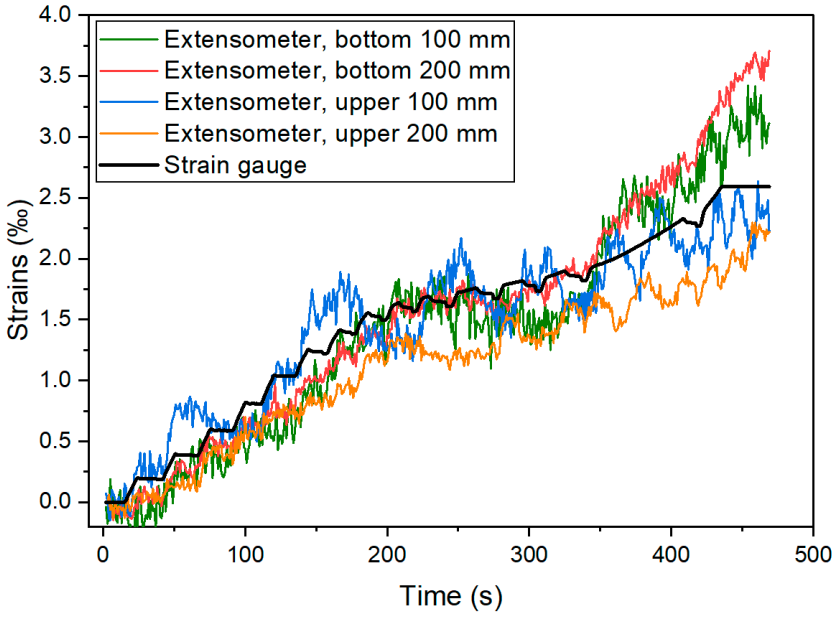


Figure 23. Comparison of the strain measurements in the plastic range in the α-α section.

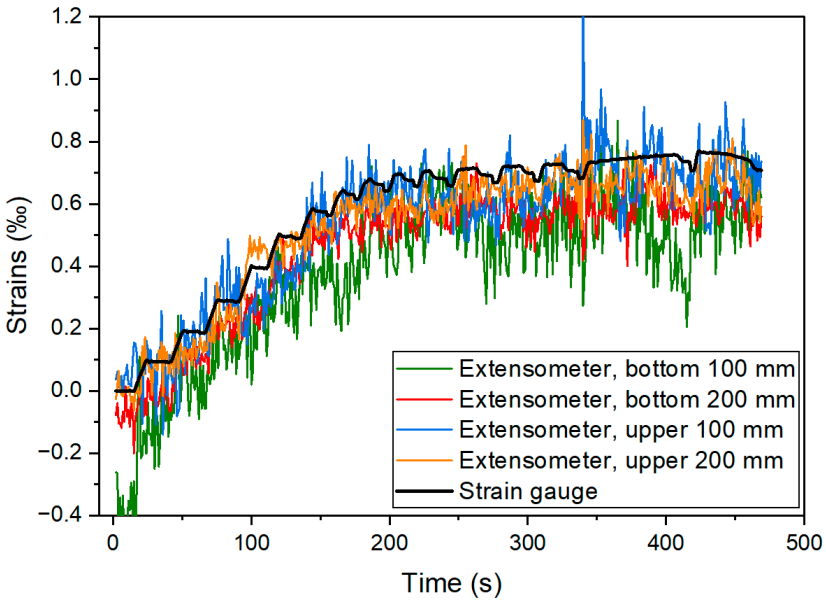


Figure 24. Comparison of the strain measurements in the plastic range in the β-β section.

In order to correctly interpret the conclusions presented above, it should be remembered that they concern measurements on a steel structure. So, a material with high stiffness (high value of Young's modulus), and then high plastic deformation capacity. In the case

of measurements on elements made of brittle materials such as concrete, the DIC system is well suited. This system enables a very effective measurement of crack propagation, as shown, for example, in [31–33]. This is due to the appearance of much larger values of displacements between the pattern points.

4. Discussion

The present research study tested the usefulness of various measurement techniques in civil engineering, particularly in terms of displacement and strain. The classic methods traditionally used in industrial practice were compared with new techniques that are becoming more popular. The classic approach in displacement measurement covered LVDTs manufactured by HBM. Electrical resistance strain gauges were the classic technique used for strain measurement. The laser scanning (FARO Focus S70) and digital image correlation (ARAMIS SRX 3D) provided the more modern alternatives.

The comparison of obtained results proved to be very interesting. Relative to their size, civil engineering structures are characterized with small displacement and strain values. For structural steel, a strain value of 1–2‰ corresponds to reaching the yield point. Therefore, the fact that very small physical values had to be measured demonstrated very well both the advantages and disadvantages of the successive measurement methods.

In displacement measurement, all the methods performed well. Satisfactory accuracy was obtained for small and large displacement and thus all methods proved to be capable of being applied in civil engineering.

The advantage of the laser scanner and DIC system is the possibility of taking measurement in many points at the same time. That feature can be used to generate beam deflection lines. The DIC system performed in that task very well, but the laser scanner had some difficulty to use the data point cloud. Measurement taken with the scanner was very noisy and consequently the deflection lines were of poor quality. It should be emphasized that the quality of deflection line very much depended on the way the scanner was positioned relative to the object. In the experiment conducted in this study, displacement was measured in the plane parallel to the beam's displacement. When the scanner was moved so that it could scan the plane perpendicular to the beam's displacement, the quality of measurement greatly improved. This is due to the fact that an average value can be calculated from the whole scanned plane.

Strain measurement proved to be interesting and exciting. Electrical resistance strain gauges performed the best. They are very sensitive and fixed to the examined object. Owing to that, strain can be measured with high accuracy down to a couple of places after a decimal point of a per mill. Measurements taken with a laser scanner and DIC system were required to create special extensometers. Strain was measured at the predefined distances of 100 and 200 mm. Finally, scanner measurement was rejected due to the very high scatter of results. Measurement with a DIC system did not produce satisfactory results either. The data spread was significant and at times it exceeded the measured values. Based on obtained results, a conclusion can be made that non-contact measurement systems cannot perform as well as electrical resistance strain gauges.

Another important thing is the difference in measurement data acquisition. The obvious advantage of strain gauges, LVDTs and a DIC system is the ability of continuous data recording at any speed. The capacity of the computer used for the process seems to be the only constraint. Measurement taken with the scanner requires more time and constant displacement of the measured object. On the other hand, laser scanning enables one to create a cloud of data points of very complicated civil engineering objects, which is a great advantage of this method.

In addition to the measuring capabilities of each of the techniques, it is also necessary to take into account the technical capabilities of the measurement. Each of these techniques has certain limitations. The assembly of strain gauges requires careful preparation of the substrate. In addition, manufacturers of adhesives for strain gauges take a 24 h wait between gluing and measuring. The measurement system should also be prepared by

creating a Wheatstone bridge. All this means that strain gauge measurements, although very precise, require a lot of work and time. LVDT sensors, similar to strain gauges, require a power supply. In addition, suitable support elements enabling contact with the specified object are also needed. Although the time needed to prepare the LVDT sensor for operation is short. Measurements with the DIC system are great in the laboratory. However, difficulties arise when measurements are required on the construction site. After each transport and installation of the cameras, calibration is required. To measure the entire surface of the object, a pattern must be made. This, again, requires preparation, which is not always possible, then only the measurement with the measuring points is left. Many of these problems do not involve a laser scanner. It works powered by a battery, it is small and it does not need direct contact with the tested object. However, it cannot measure displacements continuously.

There is also the question of costs. The most expensive solution is the equipment that enables DIC-3D measurements. The laser scanner is slightly cheaper. The most affordable solution is to use traditional methods such as strain gauges and LVDT sensors. Although, in this area, everything depends on the individual situation.

Author Contributions: Conceptualization, P.S. and P.K.; methodology, P.S. and P.K.; software, P.S. and P.K.; validation, P.S. and P.K.; writing—original draft preparation, P.K.; writing—review and editing, P.S. All authors have read and agreed to the published version of the manuscript.

Funding: This research received no external funding.

Institutional Review Board Statement: Not applicable.

Informed Consent Statement: Not applicable.

Data Availability Statement: Data sharing is not applicable to this article.

Conflicts of Interest: The authors declare no conflict of interest.

References

1. Jarosińska, M.; Berczyński, S. Changes in frequency and mode shapes due to damage in steel–concrete composite beam. *Materials* **2021**, *14*, 6232. [CrossRef] [PubMed]
2. Wróblewski, T.; Jarosińska, M.; Abramowicz, M.; Berczyński, S. Experimental validation of the use of energy transfer ratio (ETR) for damage diagnosis of steel-concrete composite beams. *J. Theor. Appl. Mech.* **2017**, *55*, 241–252. [CrossRef]
3. Wierzbicki, K.; Szewczyk, P.; Paczkowski, W.; Wróblewski, T.; Skibicki, S. Torsional stability assessment of columns using photometry and FEM. *Buildings* **2020**, *10*, 162. [CrossRef]
4. Paczkowski, W.; Wróblewski, T.; Skibicki, S. Skanowanie laserowe stalowej konstrukcji elektrowni węglowej. *Builder* **2020**, *273*, 22–25. [CrossRef]
5. De Pauw, J.; De Waele, W.; Hojjati-Talemi, R.; De Baets, P. On the use of digital image correlation for slip measurement during coupon scale fretting fatigue experiments. *Int. J. Solids Struct.* **2014**, *51*, 3058–3066. [CrossRef]
6. Lingga, B.A.; Apel, D.B.; Sepehri, M.; Pu, Y. Assessment of digital image correlation method in determining large scale cemented rockfill strains. *Int. J. Min. Sci. Technol.* **2019**, *29*, 771–776. [CrossRef]
7. Farahani, B.V.; Barros, F.; Sousa, P.J.; Cacciari, P.P.; Tavares, P.J.; Futai, M.M.; Moreira, P. A coupled 3D laser scanning and digital image correlation system for geometry acquisition and deformation monitoring of a railway tunnel. *Tunn. Undergr. Sp. Technol.* **2019**, *91*, 102995. [CrossRef]
8. Dvořák, M.; Chlup, H.; Horný, L.; Růžička, M. Comparison of strain measurement methods: Optical FBG sensors, strain gages & digital image correlation. In Proceedings of the EAN 2012 Proceedings of the 50th Annual Conference on Experimental Stress Analysis, Tabor, Czech Republic, 4–7 June 2012.
9. Dizaji, M.S.; Harris, D.K.; Kassner, B.; Hill, J.C. Full-field non-destructive image-based diagnostics of a structure using 3D digital image correlation and laser scanner techniques. *J. Civ. Struct. Health Monit.* **2021**, *11*, 1415–1428. [CrossRef]
10. Paper, C. Validation of a Structural Health and Loads Monitoring Platform Using Digital Image Correlation. In Proceedings of the 27th ICAF Symposium, Jerusalem, Israel, 5–7 June 2013; pp. 5–7.
11. Beizaee, S.; William, K.J.; Xotta, G.; Mousavi, R. Error Analysis of Displacement Gradients via Finite Element Approximation of Digital Image Correlation System. In Proceedings of the 9th International Conference on Fracture Mechanics of Concrete and Concrete Structures, Berkeley, CA, USA, 28 May–1 June 2016.
12. Lopes, J.; Stefaniak, D.; Reis, L.; Camanho, P.P. Single lap shear stress in hybrid CFRP/Steel composites. *Procedia Struct. Integr.* **2016**, *1*, 58–65. [CrossRef]

13. Sendrowicz, A.; Myhre, A.O.; Wierdak, S.W.; Vinogradov, A. Challenges and accomplishments in mechanical testing instrumented by in situ techniques: Infrared thermographydigital image correlation, and acoustic emission. *Appl. Sci.* **2021**, *11*, 6718. [CrossRef]
14. Żaba, K.; Trzepieciński, T.; Puchlerska, S.; Noga, P.; Balcerzak, M. Coupled thermomechanical response measurement of deformation of nickel-based superalloys using full-field digital image correlation and infrared thermography. *Materials* **2021**, *14*, 2163. [CrossRef]
15. Hoffmann, K. *An Introduction to Stress Analysis and Transducer Design Using Strain Gauges*. 2012. Available online: www.hbm.com (accessed on 16 November 2021).
16. Sjödahl, M. Gradient correlation functions in digital image correlation. *Appl. Sci.* **2019**, *9*, 2127. [CrossRef]
17. Shadmehri, F.; Van Hoa, S. Digital image correlation applications in composite automated manufacturing, inspection, and testing. *Appl. Sci.* **2019**, *9*, 2719. [CrossRef]
18. Lahtinen, T.; Vilaça, P.; Peura, P.; Mehtonen, S. MAG Welding tests of modern high strength steels with minimum yield strength of 700 MPa. *Appl. Sci.* **2019**, *9*, 1031. [CrossRef]
19. Welded, U.; Using, J. Determination of the Actual Stress—Strain Diagram for Undermatching Welded Joint Using DIC and FEM. *Materials* **2021**, *14*, 4691. [CrossRef]
20. Mani, C.; Balasubramani, S.; Karthikeyan, R.; Kannan, S. Digital image correlation of tensile properties for monel 400/SS 316L dissimilar metal welding joints. *Materials* **2021**, *14*, 1560. [CrossRef]
21. Wang, Y.; Ueda, K.; Nagao, R.; Tsutsumi, S. Measurements Using DIC and XRD. *Materials* **2021**, *14*, 5802. [CrossRef]
22. Żaba, K.; Trzepieciński, T.; Rusz, S.; Puchlerska, S.; Balcerzak, M. Full-field temperature measurement of stainless steel specimens subjected to uniaxial tensile loading at various strain rates. *Materials* **2021**, *14*, 5259. [CrossRef]
23. Javaid, M.; Haleem, A.; Pratap Singh, R.; Suman, R. Industrial perspectives of 3D scanning: Features, roles and it's analytical applications. *Sens. Int.* **2021**, *2*, 100114. [CrossRef]
24. Helle, R.H.; Lemu, H.G. A case study on use of 3D scanning for reverse engineering and quality control. *Mater. Today Proc.* **2021**, *45*, 5255–5262. [CrossRef]
25. Vagovský, J.; Buranský, I.; Görög, A. Evaluation of measuring capability of the optical 3D scanner. *Procedia Eng.* **2015**, *100*, 1198–1206. [CrossRef]
26. Garbowski, T.; Knitter-Piątkowska, A.; Marek, A. New edge crush test configuration enhanced with full-field strain measurements. *Materials* **2021**, *14*, 5768. [CrossRef] [PubMed]
27. Almazán-Lázaro, J.A.; López-Alba, E.; Rubio-García, L.; Díaz-Garrido, F.A. Indentation measurement in thin plates under bending using 3d digital image correlation. *Appl. Sci.* **2021**, *11*, 2706. [CrossRef]
28. Bilko, P.; Skoratko, A.; Rutkiewicz, A.; Małyszko, L. Determination of the shear modulus of pine wood with the arcan test and digital image correlation. *Materials* **2021**, *14*, 468. [CrossRef] [PubMed]
29. Malowany, K.; Piekarczuk, A.; Malesa, M.; Kujawińska, M.; Wiech, P. Application of 3D digital image correlation for development and validation of FEM model of self-supporting arch structures. *Appl. Sci.* **2019**, *9*, 1305. [CrossRef]
30. Blenkinsopp, R.; Roberts, J.; Harland, A.; Sherratt, P.; Smith, P.; Lucas, T. A method for calibrating a digital image correlation system for full-field strain measurements during large deformations. *Appl. Sci.* **2019**, *9*, 2828. [CrossRef]
31. Beßling, M.; Czaderski, C.; Orlowsky, J. Prestressing effect of shape memory alloy reinforcements under serviceability tensile loads. *Buildings* **2021**, *11*, 101. [CrossRef]
32. Pająk, M.; Wandzik, G. Laboratory tests of concrete beams reinforced with recycled steel fibres and steel bars. *Materials* **2021**, *14*, 6752. [CrossRef]
33. Krassowska, J.; Kosior-Kazberuk, M. The effect of steel and basalt fibers on the shear behavior of double-span fiber reinforced concrete beams. *Materials* **2021**, *14*, 6090. [CrossRef]